High shunt resistance in polymer solar cells comprising a MoO3 hole extraction layer processed from nanoparticle suspension

Tobias Stubhan, Tayebeh Ameri, Michael Salinas, Johannes Krantz, Florian Machui et al.

Citation: Appl. Phys. Lett. **98**, 253308 (2011); doi: 10.1063/1.3601921
View online: http://dx.doi.org/10.1063/1.3601921
View Table of Contents: http://apl.aip.org/resource/1/APPLAB/v98/i25
Published by the American Institute of Physics.

High shunt resistance in polymer solar cells comprising a MoO_3 hole extraction layer processed from nanoparticle suspension

Tobias Stubhan,[1,a)] Tayebeh Ameri,[1] Michael Salinas,[2] Johannes Krantz,[1] Florian Machui,[1] Marcus Halik,[2] and Christoph J. Brabec[1,3]
[1]*Institute of Materials for Electronics and Energy Technology (I-MEET), Friedrich-Alexander-University of Erlangen-Nuremberg, Martensstraße 7, 91058 Erlangen, Germany*
[2]*Organic Materials and Devices (OMD), Institute of Polymer Materials, Friedrich-Alexander-University of Erlangen-Nuremberg, Martensstraße 7, 91058 Erlangen, Germany*
[3]*Bavarian Center for Applied Energy Research (ZAE Bayern), Am Weichselgarten 7, 91058 Erlangen, Germany*

(Received 3 May 2011; accepted 13 May 2011; published online 24 June 2011)

In this report, we present solution processed molybdenum trioxide (MoO_3) layers incorporated as hole extraction layer (HEL) in polymer solar cells (PSCs) and demonstrate the replacement of the commonly employed poly(3,4-ethylene dioxythiophene):(polystyrene sulfonic acid) (PEDOT:PSS). MoO_3 is known to have excellent electronic properties and to yield more stable devices compared to PEDOT:PSS. We demonstrate fully functional solar cells with up to 65 nm thick MoO_3 HEL deposited from a nanoparticle suspension at low temperatures. The PSCs with an active layer comprising a blend of poly(3-hexylthiophene) and [6,6]-phenyl-C_{61} butyric acid methyl ester and a MoO_3 HEL show comparable performance to reference devices with a PEDOT:PSS HEL. The best cells with MoO_3 reach a fill factor of 66.7% and power conversion efficiency of 2.92%. Moreover, MoO_3 containing solar cells exhibit an excellent shunt behavior with a parallel resistance of above 100 $k\Omega\,cm^2$. © *2011 American Institute of Physics*. [doi:10.1063/1.3601921]

During the past decade, fast progress has happened in the field of organic photovoltaics.[1] Polymer solar cells (PSCs) now offer a promising approach for a low-cost and flexible photovoltaic technology. Significant advances have led to certified efficiencies of 8.3% (Refs. 2 and 3) and respectively 9.2% (Ref. 4) and expectations are that the magic 10% hurdle will be overcome soon. Before widespread commercialization, large area production, and stability issues have to be solved.

The "working horse" material employed as solution processed hole extraction layer (HEL) for organic photovoltaics is poly(3,4-ethylene dioxythiophene):(polystyrene sulfonic acid) (PEDOT:PSS). Unfortunately, PEDOT:PSS is identified as a major source of degradation in standard architecture PSCs (inset of Fig. 1) due to its acidic and hygroscopic nature.[5–7] A frequently employed strategy to solve this issue is to invert the layer sequence. Inverted architectures find PEDOT:PSS sandwiched between the organic semiconductor and a more stable back electrode, such as Ag or Au.[8] The active layer surfaces often have a very low surface energy [e.g., poly(3-hexylthiophene):[6,6]-phenyl-C_{61} butyric acid methyl ester (P3HT:PCBM) in ratio 1:1 only ~25 mN/m], which makes it very difficult to coat water-based solutions like conventional PEDOT:PSS formulations on top. Furthermore, it is a big advantage to be able to choose the architecture, that suits the vertical phase separation of the used organic photovoltaic material best.[9,10] Ultimately, employing the normal layer sequence and just replacing PEDOT:PSS through a more stable alternative is a promising approach to solve this stability issue.

Materials for a stable hole selective contact are transition metal oxides such as MoO_3,[11,12] WO_3,[13] V_2O_5,[12] and NiO.[14] Among these, MoO_3 is one of the most interesting materials, because of its nontoxic nature and the very deep lying electronic states.[15] Various groups have shown that comparable device performance and increased lifetime can be achieved with evaporated MoO_3 ($eMoO_3$) as PEDOT: PSS replacement.[5,9,11] From the perspective of large scale production, the frequently employed vacuum process for deposition and the limited layer thickness are two major disadvantages of MoO_3.[5] Recently, solution processed MoO_3 layers from precursor solution[11] as well as from a commercially available nanoparticle dispersion[15] were reported. Especially the layers deposited from nanoparticle dispersion appear attractive, since they offer electronic properties comparable to $eMoO_3$, while keeping the advantage of low temperaure solution deposition they offer electronic properties comparable to $eMoO_3$ while at the same time having the advantage of low

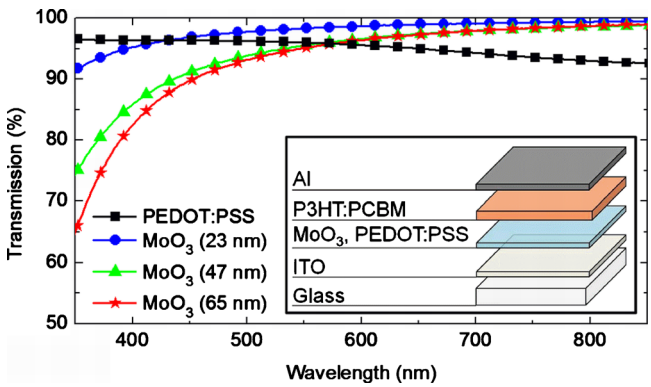

FIG. 1. (Color online) Transmission of solution processed MoO_3 vs the PEDOT:PSS reference. The inset shows the layer stack of the investigated solar cells.

[a)]Author to whom correspondence should be addressed. Electronic mail: tobias.stubhan@ww.uni-erlangen.de. Tel.: ++49 (0)9131-852 7634. FAX: ++49 (0)9131-852 8495.

temperature deposition (max. 100 °C).[15] In this letter, we incorporated MoO_3 layers processed from this nanoparticle suspension as HEL in PSCs.

The devices were processed in ambient atmosphere. Prestructured indium tin oxide (ITO) coated glass substrates (Osram) were cleaned in acetone and isopropyl alcohol. After drying, the substrates were coated with the HEL. The MoO_3 suspension (5 wt %, surfactant stabilized by an undisclosed block copolymer in xylene), obtained from Nanograde Llc. (Product No. 3007), was deposited via doctor blading from diluted dispersion (0.5–2 wt %). The further treatment followed a method described by Meyer *et al.*[15] Afterwards, the samples were baked on a hot plate at 100 °C for 10 min. To remove the dispersing agent, the samples were treated in an O_2-plasma (2 min, 200 W, 0.2 mbar, gas flow 3 sccm). An approx. 50 nm thick PEDOT:PSS (VP Al 4083) from H.C. Starck layer was deposited for reference devices. An approx. 100 nm thick active layer was doctor bladed from a 2 wt % chlorobenzene solution of P3HT (Merck) and technical grade PCBM (Solenne). The whole stack was annealed on a hot plate at 140 °C for 5 min after evaporation of a 100 nm thick Al layer to form the top electrode. The active area was 10.4 mm^2. Current density-voltage (j-V) characteristics were measured with a source measurement unit from BoTest. Illumination was provided by an OrielSol 1A Solar simulator with AM1.5G spectra at 0.1 W/cm^2.

The solution processed MoO_3 was investigated in three different layer thickness of app. 23, 47, and 65 nm. As reference, an approx. 50 nm PEDOT:PSS layer was used. Figure 1 shows the transmission of the four layers. MoO_3 starts absorbing weakly in the blue. For the longer wavelengths, the transmission of all four layers is comparable and high (>90%).

The j-V characteristics of the solar cells incorporating the four different HELs are shown in Fig. 2, and the corresponding key parameters are listed in Table I. The solar cells with MoO_3 layers show a trend as a function of film thickness. The fill factor (FF) and the open circuit voltage (V_{OC}) increase slightly with layer thickness from 54.6 to 61.5% for the FF and 547 to 579 mV for the V_{OC}. This increase is explained by a decreasing saturation current density (j_0) with thicker MoO_3 layers as obtained via simulation of the j-V characteristics using a method described by Waldauf *et al.*[16] However, the main impact on the device performance can be attributed to the short circuit current density (j_{SC}). The solar cell with a 47 nm thick MoO3 layer shows a j_{SC} of −7,61 mA/cm^2 while the other two configurations only show −6.76 mA/cm^2 (23 nm) and −6.79 mA/cm^2 (65 nm).

Three effects were identified which influence the j_{SC} change as a function of MoO_3 layer thicknesses. One contribution arises from optical losses due to absorbed photons in the different HELs. Table I gives an overview on the roughly estimated absorption losses in the HELs. The differences qualitatively do not correlate with the measured data. Next, we analyzed the losses from serial resistance (R_S). The R_S of the devices incorporating the two thinner MoO_3 layers is more or less identical at around 1 Ω cm^2 and well within expectations. This is a proof that the contribution of the HEL to the R_S of the device is negligible for these thicknesses. The contribution of the MoO_3 layer to the R_S becomes perceptible for the 65 nm film, and it increases to 3 Ω cm^2.

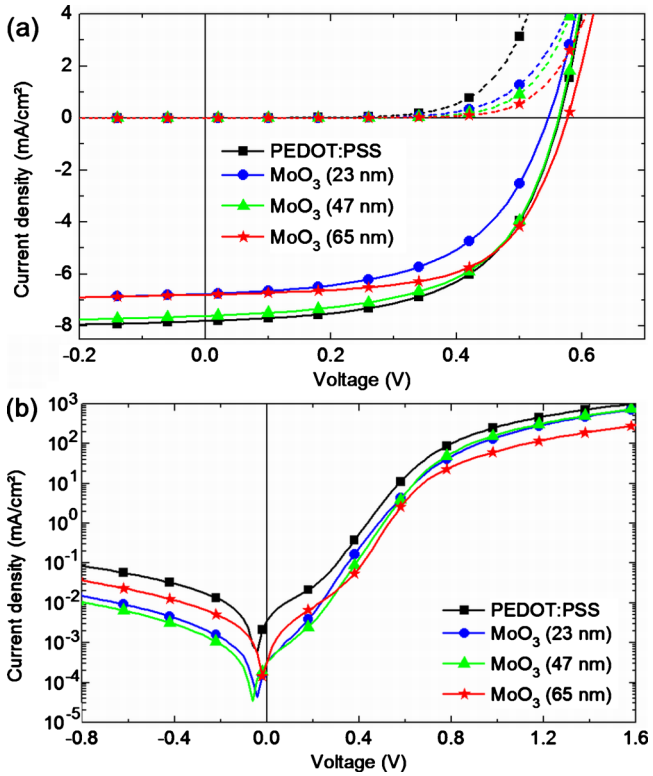

FIG. 2. (Color online) (a) Averaged j-V characteristics of solar cells with solution processed MoO_3 vs PEDOT:PSS HELs (b) corresponding logarithmic plot of dark j-V characteristics.

Such high R_S can explain a small part of the j_{SC} reduction observed for the thick MoO_3 devices. However, in general the series resistance values are far too low to explain the j_{SC} trend. This is particularly true for the thin MoO_3 layers. The third and probably most prominent influence on j_{SC} is deduced from the Figs. 3(a)–3(f), showing the AFM images of the three MoO_3 layers. The layer with the mean thickness of 23 nm [Fig. 3(a)] shows low coverage and quite significant particle agglomeration leading to a high pinhole density and surface roughness (Rms=27 nm). The 47 nm film exhibits the best homogeneity among the three layers with the lowest pinhole density and surface roughness (Rms=15 nm). The thicker film (~65 nm) again shows higher defect density and surface roughness (Rms=30 nm). The AFM images of the surfaces of the P3HT:PCBM films covering the MoO_3 layers are depicted in Figs. 3(d)–3(f). It is observed that some agglomerates even poke through the subsequently deposited active layer for the 23 and 65 nm thick films. Even though the 47 nm thick film that exhibits the best morphology is not free from defects, the P3HT:PCBM film apparently evens out the surface of MoO_3 quite efficiently and the Rms value of the P3HT:PCBM surface is low with only 3 nm [see Fig. 3(e)]. With respect to this information, interface (direct contact of active layer and ITO electrode) and active layer shunts are expected. Counter-intuitively, the shunt resistance (R_{Shunt}) of all the MoO_3 containing devices is very high with values of up to 107 kΩ cm^2 (47 nm film). The R_{Shunt} is found to be 73 kΩ cm^2 even for the 23 nm film and still 36 kΩ cm^2 for the 65 nm film. These values are much better than the 14 kΩ cm^2 of the PEDOT:PSS reference device. From that we can conclude that MoO_3 based devices do not suffer from shunting. Coming back to the j_{SC} losses, we suggest that the area where MoO_3 pokes into or even through

TABLE I. Averaged data of at least five cells from one substrate of a representative run is displayed. "Overall best" means best cell from seven runs.

	V_{OC} (mV)	PCE (%)	FF (%)	j_{SC} (mA/cm^2)	j_{SC} change due to optical losses[a] (%)	R_S (Ω cm^2)	R_{Shunt} (kΩ cm^2)
PEDOT:PSS	563	2.53	57.4	−7.81	−4	0.8	14
sMoO_3 (23 nm)	547	2.02	54.6	−6.76	−3	1.1	73
sMoO_3 (47 nm)	558	2.47	58.0	−7.61	−9	1.1	107
sMoO_3 (65 nm)	579	2.42	61.5	−6.79	−11	3.0	36
Overall best PEDOT:PSS	580	3.23	62.2	−8.96			
Overall best MoO_3 (47 nm)	570	2.92	66.7	−7.67			

[a]Simple optical modeling, only considering single pass absorption in the HEL without taking thin film interference and reflection into account.

the active layer has a reduced photocurrent production. This would coincide qualitatively with the trend for the measured j_{SC}. In summary, we have identified three different loss mechanisms, which can potentially explain the tendency to lesser photocurrent. Surface roughness, incomplete coverage and optical losses may be responsible for this observation. In addition, it is important to note that an increased active layer thickness may reverse this trend.

Overall, the best devices incorporating 47 nm thick MoO_3 films show comparable performance to the PEDOT:PSS reference devices (see Table I). According to the experiments until now, the j_{SC} of the MoO_3 devices is found to be generally equal or slightly lower than the j_{SC} of the PEDOT:PSS devices. In our experiments, we could observe MoO_3 devices with FFs of up to 66.7% and PCE′s of 2.92% while the best PEDOT:PSS device reached 62.2 and 3.23%.

In this report, we demonstrated solution processed MoO_3 as a promising stable alternative to PEDOT:PSS. The MoO_3 films can be deposited from nanoparticle solution at low temperatures and reasonable thickness of up to 65 nm without reducing the device performance significantly. Furthermore, devices incorporating MoO_3 layers show very high R_{Shunt} values of up to over 100 kΩ cm^2, thus clearly outperforming the PEDOT:PSS reference. The high R_{Shunt} allows for maintaining the high PCE also at low light intensity conditions, which is very important for all indoor and mobile applications.[17] Further investigations on a method to deposit these particles without an oxygen plasma posttreatment are necessary.

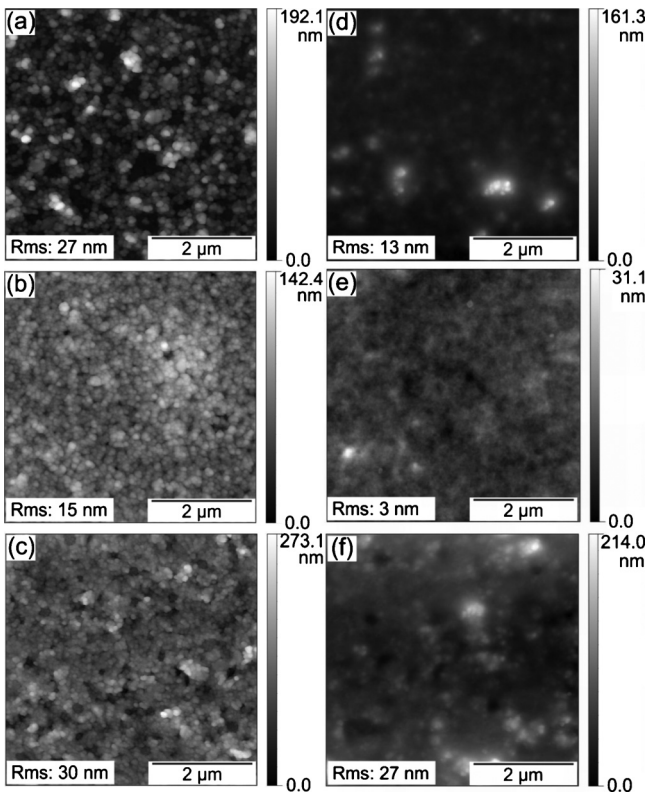

FIG. 3. AFM images of 23 nm [(a) and (d)], 47 nm [(b) and (e)] and 65 nm [(c) and (f)] thick MoO_3 films on ITO. For [(d)–(f)] the layers are covered with a ca. 100 nm thick active layer.

The authors gratefully acknowledge the support of the Cluster of Excellence "Engineering of Advanced Materials" at the University of Erlangen-Nuremberg, which is funded by the German Research Foundation (DFG) within the framework of its "Excellence Initiative." This work was funded by a German Research Foundation project grant (DFG; Grant No. BR 4031/1-1).

[1]C. J. Brabec, S. Gowrisanker, J. J. M. Halls, D. Laird, S. Jia, and S. P. Williams, Adv. Mater. (Weinheim, Ger.) **22**, 3839 (2010).
[2]Heliatek. Available at: HYPERLINK http://www.heliatek.com.
[3]Konarka. Available at: HYPERLINK http://www.konarka.com/.
[4]R. F. Service, Science **332**, 293 (2011).
[5]E. Voroshazi, B. Verreet, A. Buri, R. Müller, D. D. Nuzzo, and P. Heremans, Org. Electron. **12**, 736 (2011).
[6]M. Jørgensen, K. Norrman, and F. C. Krebs, Sol. Energy Mater. Sol. Cells **92**, 686 (2008).
[7]K. Norrman, S. A. Gevorgyan, and F. C. Krebs, ACS Appl. Mater. Interfaces **1**, 102 (2009).
[8]R. Steim, S. A. Choulis, P. Schilinsky, and C. J. Brabec, Appl. Phys. Lett. **92**, 093303 (2008).
[9]Y. Sun, J. H. Seo, C. J. Takacs, J. Seifter, and A. J. Heeger, Adv. Mater. (Weinheim, Ger.) **23**, 1679 (2011).
[10]W. Cai, X. Gong, and Y. Cao, Sol. Energy Mater. Sol. Cells **94**, 114 (2010).
[11]F. Liu, S. Shao, X. Guo, Y. Zhao, and Z. Xie, Sol. Energy Mater. Sol. Cells **94**, 842 (2010).
[12]V. Shrotriya, G. Li, Y. Yao, C. W. Chu, and Y. Yang, Appl. Phys. Lett. **88**, 073508 (2006).
[13]C. Tao, S. Ruan, G. Xie, X. Kong, L. Shen, F. Meng, C. Liu, X. Zhang, W. Dong, and W. Chen, Appl. Phys. Lett. **94**, 043311 (2009).
[14]K. X. Steirer, J. P. Chesin, N. E. Widjonarko, J. J. Berry, A. Miedaner, D. S. Ginley, and D. C. Olson, Org. Electron. **11**, 1414 (2010).
[15]J. Meyer, R. Khalandovsky, P. Görrn, and A. Kahn, Adv. Mater. (Weinheim, Ger.) **23**, 70 (2011).
[16]C. Waldauf, P. Schilinsky, J. Hauch, and C. J. Brabec, Thin Solid Films **451**, 503 (2004).
[17]R. Steim, T. Ameri, P. Schilinsky, C. Waldauf, G. Dennler, M. Scharber, and C. J. Brabec, Sol. Energy Mater. Sol. Cells (to be published).